

# DFT Study of 4-Acetamido-N-(3-amino-1,2,4-triazol-1-yl) Benzene Sulfonamide and its Potential Application as Copper Corrosion Inhibitor

A.I. Aljameel

Department of physics, College of Science, Imam Mohammad Ibn Saud Islamic University (IMSIU), 11623 Riyadh, Saudi Arabia

E-mail: [aialjameel@imamu.edu.sa](mailto:aialjameel@imamu.edu.sa)

Received: 24 January 2022/ Accepted: 11 March 2022 / Published: 5 April 2022

This study provides a theoretical investigation into the inhibition efficiency of 4-acetamido-N-(3-amino-1,2,4-triazol-1-yl) benzenesulfonamide. The molecule was previously synthesized unintentionally in an attempt to fabricate copper corrosion inhibitors. Density functional theory (DFT) concepts were used to model the molecule's molecular structure and electronic properties. In comparison to compounds with similar molecular structures, calculated global reactivity indices such as the highest occupied molecular orbital–lowest unoccupied molecular orbital (HOMO-LUMO) energy gap (4.71 eV), chemical hardness (2.36 eV), and softness (0.42 eV) revealed high chemical reactivity for the title inhibitor. Further, the geometrical parameters of the ground state molecular structure were computed and compared to experimental data. The molecule's high susceptibility to electron transfer via the interacting species was disclosed by analyzing the HOMO and LUMO. As indicated by the molecular electrostatic potential map and Mulliken charge analysis, the lateral distribution of active sites for nucleophilic and electrophilic attacks, as well as negative charges, endows the molecule with high inhibition capability. The partial density of states (PDOS) spectra revealed the most influential molecular orbital in the electronic properties of the inhibitor. According to the findings, the proposed molecule has a high level of chemical reactivity, making it a promising copper corrosion inhibitor.

**Keywords:** Corrosion Inhibitor; Geometrical Parameters; MEP; Mulliken Charges; PDOS.

## 1. INTRODUCTION

Corrosion inhibitors have become a highly effective and economical method of preventing copper corrosion due to their mature technology and outstanding performance against corrosion [1], one of the most serious problems in the industrial sector, which causes grievous casualties and enormous property loss [2, 3]. Corrosion is defined as the degradation of a metal's surface due to a

chemical reaction with the surroundings, and it is one of the most widely researched phenomena in the last few decades.

Several studies have explored the optimum methods of coating metal surfaces with organic or inorganic materials as a protection in various media [4–6], and it has been discovered that the use of corrosion inhibitors is one of the cheapest and most effective techniques for corrosion prevention. Inorganic composites specified as chromates, nitrates, oxides, and lanthanides have been utilized as common inhibitors for corrosion [7–10].

Copper is a relatively noble metal, resistant to the influence of the atmosphere and many chemicals, requiring strong oxidants for its corrosion or dissolution. However, it is known that, in aggressive media, it is susceptible to corrosion [11–14]. Thus, copper corrosion inhibitors are necessary since no passive protective layer can be expected to form [15–20]. Although experimental techniques are instrumental in understanding inhibition mechanisms, they have some limitations, such as being time-consuming and highly costly [21, 22].

Of late, the theoretical approach represented by density functional theory (DFT) has become a powerful tool in studying the inhibition properties of molecules [23–27]. DFT concepts have a huge capability to interpret and predict the inhibition performance of organic and inorganic inhibitors based on the reactivity indexes and electronic and molecular properties [28–30].

This work investigated the inhibition efficiency of a novel molecule, 4-acetamido-N-(3-amino-1,2,4-triazol-1-yl)benzenesulfonamide, which was previously synthesized in an attempt to treat copper corrosion as an active inhibitor. DFT means were used to determine the structural quantum parameters of these compounds and classify their inhibition efficiency according to the calculated molecular properties

## 2. MATERIALS and METHODS

### 2.1. Experimental Details

The proposed molecule, 4-acetamido-N-(3-amino-1,2,4-triazol-1-yl)benzenesulfonamide, was unintentionally produced by the Fu Juan group while attempting to treat copper corrosion by synthesizing an active inhibitor using p-acetylaminobenzenesulfonyl chloride and 3-Amino-1-H-1,2,4-triazole [31]. Figure 1(A) illustrates the molecular structure of the title molecule,  $C_{10}H_{11}N_5O_3S$ .

Because it contains many heteroatoms, the group anticipated that the title molecule would be a promising copper corrosion inhibitor that would easily interact with copper to form a coating complex. The mentioned work includes a detailed description of the synthesis method as well as supplementary materials that clearly define the refinement, fractional atomic coordinates, equivalent isotropic displacement, and geometric parameters for the title molecule.

### 2.2. Computational Methods

The molecular structure of 4-acetamido-N-(3-amino-1,2,4-triazol-1-yl)benzenesulfonamide was investigated using DFT, which was expressed by the Becke3-parameter-Lee-Yang-Parr (B3LYP)

model and the 6-311G\*\* basis set, to find the optimized ground state [32, 33]. The calculations were conducted using the computational chemistry software package Gaussian 09 [34]. GaussView 5.0 was used to extract and visualize the surface of molecular electrostatic potential, highest occupied molecular orbital(HOMO) and lowest unoccupied molecular orbital(LUMO) energies, frontier molecular orbitals, and atomic charges [35]. The density of states (DOS) and partial density of states (PDOS) spectra were generated using the GaussSum program [36] with an FWHM of 0.3 eV, and the graphs were plotted using the origin program.

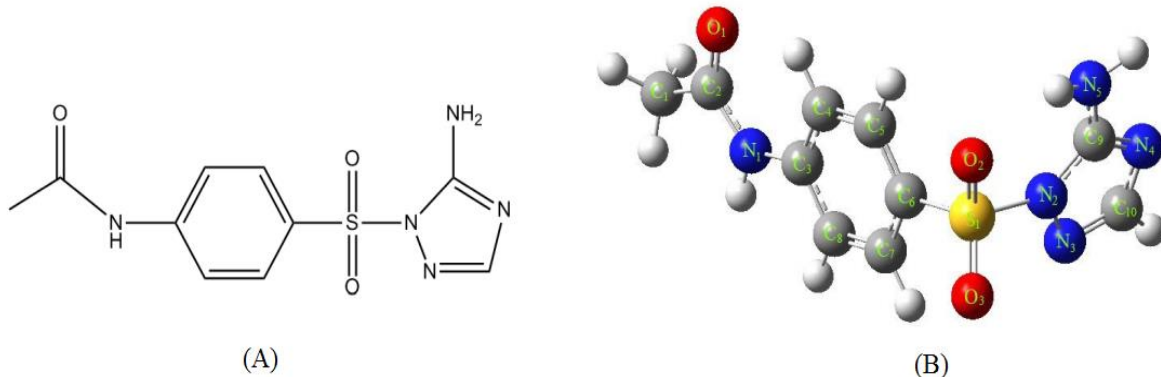


**Figure 1.** Molecular structure(A) and optimized geometry (B) of 4-Acetamido-N-(3-amino-1,2,4-triazol-1-yl)benzenesulfonamide molecule.

### 3. RESULTS

#### 3.1. Chemical reactivity descriptors

The properties and electronic structure of a molecule must be identified to describe its behavior in a chemical reaction with another chemical substance. DFT has been used successfully to investigate quantum chemical descriptors of molecular systems, which correlate molecular orbital energies to chemical reactivity. In this regard, the chemical DFT descriptors derived by Koopmans' theorem [37] were determined for the title inhibitor. These include chemical potential ( $\mu$ ), ionization potential (I), electronic affinity (A), hardness ( $\eta$ ), softness ( $\sigma$ ), electronegativity ( $\chi$ ), electrophilicity ( $\omega$ ), and the fraction of electrons transferred ( $\Delta N$ ). The mathematical representation of these chemical indices and their calculated values are recorded in Table 1.

$E_{\text{HOMO}}$  signifies the energy of the HOMO, while  $E_{\text{LUMO}}$  indicates the energy of the LUMO. The ionization potential (I) and the electron affinity (A) are denoted as  $-E_{\text{HOMO}}$  and  $-E_{\text{LUMO}}$ . The gap in the energy band reflects the reactivity of the inhibitor to the adsorption process on metal surfaces. Smaller energy gaps indicate better inhibitory activity since the energy required to remove an electron from the most occupied orbital is lesser [38].

A molecule's resistance to changes in its electronic distribution during chemical interactions is defined as hardness. Consequently, reduced hardness, or softness, indicates a comparatively polarizable molecule whose electronic distribution can be easily changed in a chemical reaction. As the hardness and softness values were low and high, respectively, for the title molecule, it meant that it is a molecule with high chemical reactivity and high corrosion inhibition efficiency.

Table 1 show that the calculated values of  $E_g$ ,  $\eta$ , and  $\sigma$  were 4.71 eV, 2.36 eV, and 0.42 eV<sup>1</sup>, respectively. Thus, compared to previously reported molecules with similar structures, the investigated inhibitor has a smaller gap in the energy band, lower hardness, and a higher softness value, indicating a good inhibition capability [39, 40].

Electronegativity is a measure of the molecule's ability to attract electrons and is a critical property in predicting the efficiencies of the molecule as a corrosion inhibitor. As per Sanderson's principle [41], electrons flow from the molecule having low electronegativity (inhibitor) to the one with the higher electronegativity (metal surface) until the values equalize and chemical equilibrium is attained. As thought, the measured electronegativity of the inhibitor is lower (4.12 eV) than that of the metal surface (copper).

Electrophilicity refers to a molecule's preference to acquire electrons from its surroundings. Based on the absolute electrophilicity criteria, the investigated inhibitor is categorized as a strong electrophile [42]. The number of electrons transferred between the inhibitor and metal surface during a chemical interaction is denoted by the numerical parameter,  $\Delta N$ . In Table 1,  $\Delta N$  was calculated using the theoretical values of electronegativity and global hardness for bulk copper as  $\chi_{Cu} = 4.98 \text{ eV}$   $\eta_{Cu} = 0$  respectively, implying that, for a metallic bulk,  $I = A$  since they are softer than neutral metallic atoms [43]. The calculated positive value of  $\Delta N$  indicated that the inhibitor behaves as an electron donor, i.e., the inhibitor's efficiency is due to electron donation.

**Table 1.** The predicted reactivity descriptors for 4-Acetamido-N-(3-amino-1,2,4-triazol-1-yl)benzene sulfonamide using B3LYP/6-311G\*\* model.

Parameter	Symbol	Mathematical Definition	This work C10H11N5O3S	Previous work C9H14N4O4S [39]	Previous work C10H12N4OS [40]
HOMO Energy	$E_{\text{HOMO}}$	_____	-6.47	-5.58	-6.58
LUMO Energy	$E_{\text{LUMO}}$	_____	-1.76	-0.57	-0.86
Energy gap	$E_g$	$E_{\text{LUMO}} - E_{\text{HOMO}}$	4.71	5.01	5.72
Ionization potential	$I$	$-E_{\text{HOMO}}$	6.47	5.58	6.58
Electron affinity	$A$	$-E_{\text{LUMO}}$	1.76	0.57	0.86
Chemical hardness	$\eta$	$\frac{I - A}{2}$	2.36	2.50	2.86
Chemical softness	$\sigma$	$\frac{1}{\eta} = \frac{1}{I - A}$	0.42	0.40	0.35
Electronegativity	$\chi$	$\frac{I + A}{2}$	4.12	3.08	3.72
Electrophilicity	$\omega$	$\frac{\chi^2}{2\eta}$	3.60	—	—
Fraction of electron transferred	$\Delta N$	$\frac{\chi_{Cu} - \chi_{inh}}{2(\eta_{Cu} + \eta_{inh})}$	0.18	—	—

### 3.2. Optimized geometric parameters

The optimized structure of the studied molecule calculated using the B3LYP technique and the 6-311G\*\* basis set is seen in Figure 1(B). Table 2 lists the calculated geometrical parameters such as bond lengths, angles, and torsion angles, along with the corresponding experimental values.

The 4-acetamido-N-(3-amino-1,2,4-triazol-1-yl)benzenesulfonamide molecule is non-planar, with the acetamido and 3-Amino-1,2,4-triazole groups forming two planes that bend at the sulfonic group. This bending is signified by the angle  $\angle N_2S_1C_6 = 103.93_{\text{Exp}}, 103.42_{\text{Cal}}$ . Other torsion angles, including C5-C6-S1-N2, C7-C6-S1-N2, C9-N2-S1-C6, N3-N2-S1-C6, etc., are shown with their values in the table.

The results of the selected geometrical parameters aligned with the experimental values, except for some parameters being slightly greater. This can be attributed to the lack of accounting for the intermolecular coulombic interaction between neighboring molecules during calculations, which were done for isolated molecules. In contrast, the experiment took this interaction into account for molecules in the crystal lattice [44].

**Table 2.** Comparison between the calculated geometrical parameters and the experimental values retrieved from the literature.

Bond length (Å)	Exp.	B3YLB /6-311**	Bond length (Å)	Exp.	B3YLB /6-311**	Angle (°)	Exp.	B3YLB /6-311**
C1-C2	1.50	1.51	O1-C2-C1	121.88	122.02	C4-C5-C6-S1	-178.89	-179.30
C2-O1	1.22	1.21	N1-C2-C1	114.44	114.20	S1-C6-C7-C8	178.12	179.50
C2-N1	1.36	1.38	C8-C3-N1	117.61	117.20	N1-C3-C8-C7	175.68	176.89
C3-N1	1.40	1.40	N1-C3-C4	122.97	123.21	O1-C2-N1-C3	-4.90	-4.81
C3-C4	1.40	1.40	C5-C4-C3	119.46	119.55	C1-C2-N1-C3	175.40	176.05
C4-C5	1.38	1.38	C4-C5-C6	120.55	119.96	C8-C3-N1-C2	170.17	171.36
C5-C6	1.38	1.39	C5-C6-C7	120.37	121.21	C4-C3-N1-C2	-12.7	-11.81
C6-C7	1.38	1.39	C5-C6-S1	120.06	119.10	N5-C9-N2-N3	176.09	176.84
C6-S1	1.75	1.77	C7-C6-S1	119.55	119.68	N4-C9-N2-S1	-175.29	-179.48
C7-C8	1.39	1.38	C7-C8-C3	120.93	120.88	N5-C9-N2-S1	3.60	3.74
C9-N4	1.32	1.32	C2-N1-C3	128.23	128.92	S1-N2-N3-C10	176.00	176.40
C9-N5	1.33	1.35	C9-N2-N3	109.16	109.42	N5-C9-N4-C10	-176.97	-176.96
C9-N2	1.38	1.38	C9-N2-S1	131.89	131.55	C9-N2-S1-O3	-152.26	-154.37
C10-N3	1.30	1.30	N3-N2-S1	118.56	119.00	N3-N2-S1-O3	35.81	36.19
C10-N4	1.36	1.36	C10-N3-N2	101.25	101.52	C9-N2-S1-O2	-23.32	-24.12
N2-S1	1.68	1.72	C9-N4-C10	103.39	103.45	N3-N2-S1-O2	164.76	165.45
O2-S1	1.42	1.45	O3-S1-O2	121.05	122.00	C9-N2-S1-C6	92.15	93.27
O3-S1	1.42	1.45	O3-S1-N2	106.64	107.46	N3-N2-S1-C6	-79.77	-78.41
N4-C9-N5	125.85	126.2	O2-S1-N2	103.89	103.20	C5-C6-S1-O3	-167.40	-166.89
N4-C9-N2	108.98	109.0	O3-S1-C6	109.43	109.28	C7-C6-S1-O3	14.06	15.77
N5-C9-N2	125.16	124.71	O2-S1-C6	110.33	109.52	C7-C6-S1-O2	-121.49	-124.84
N3-C10-N4	117.16	116.54	N2-S1-C6	103.93	103.42	C5-C6-S1-N2	-53.79	-53.67
O1-C2-N1	123.68	123.77	N1-C3-C4-C5	-176.32	-177.79	C7-C6-S1-N2	127.67	128.53

### 3.2. HOMO & LUMO Frontier Molecular Orbitals

As previously stated, HOMO and LUMO, also known as the frontier molecular orbitals, are the most valuable orbitals in organic chemical compounds. HOMO and LUMO are significant, as they represent the primary orbitals involved in chemical interactions. The ability to donate an electron is defined by HOMO, while LUMO dictates the capacity to accept an electron. Figure 2 describes the HOMO-LUMO map of the title molecule.

The HOMO distribution is confined to the 3-Amino-1,2,4-triazole group, while LUMO is found primarily on the acetamido group, with small lobes found on the triazole and the oxygen of the sulfonic group. The allocation of HOMO and LUMO on the right and left sides of the molecule further clarified the molecule's high susceptibility to charge transfer.

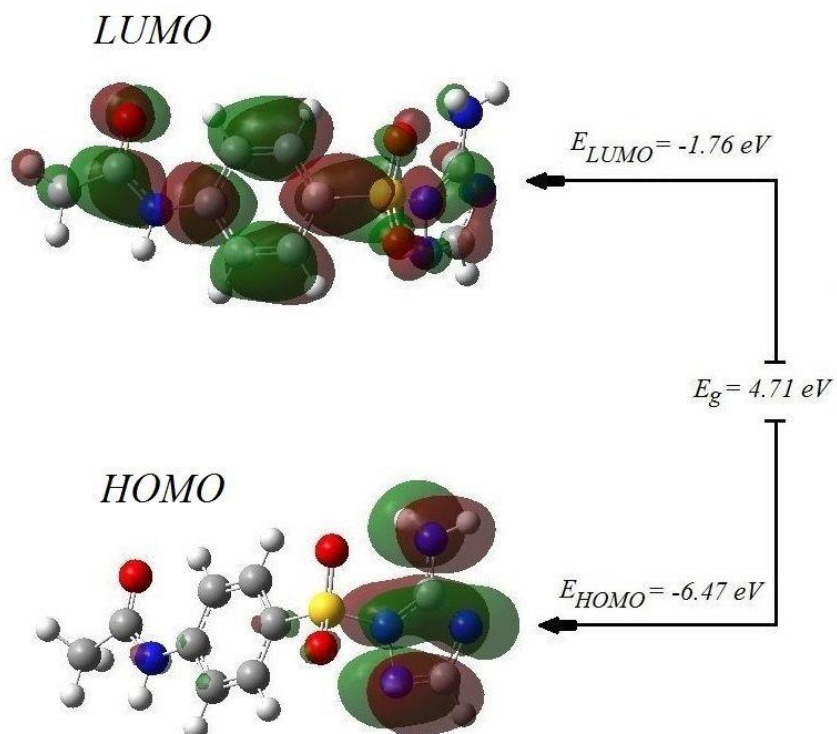


**Figure 2.** HOMO and LUMO frontier molecular orbitals diagram

### 3.3. Molecular Electrostatic Potential (MEP)

The molecular electrostatic potential (MEP) is a local descriptor that predicts chemically active regions based on nuclear and electronic charge distribution. Reactive sites for electrophilic and nucleophilic interactions are designated by a color code. The color blue indicates a positive charge region associated with an electrophilic attack, the color red represents a negative charge region associated with a nucleophilic attack, and the color green denotes electrostatic neutral potential regions. The MEP surface map is depicted in Figure 3.

The 4-acetamido-N-(3-amino-1,2,4-triazol-1-yl) benzenesulfonamide molecule has the most negative regions on the oxygen atoms of the carbonyl and sulfonic groups and the nitrogen atom of the triazole group, making them attractive sites for an electrophilic attack. Positive regions are found around the hydrogen atoms of the amino group and the lower hydrogen atoms in the acetamido group, which seem to be the most preferred locations for nucleophilic interactions.

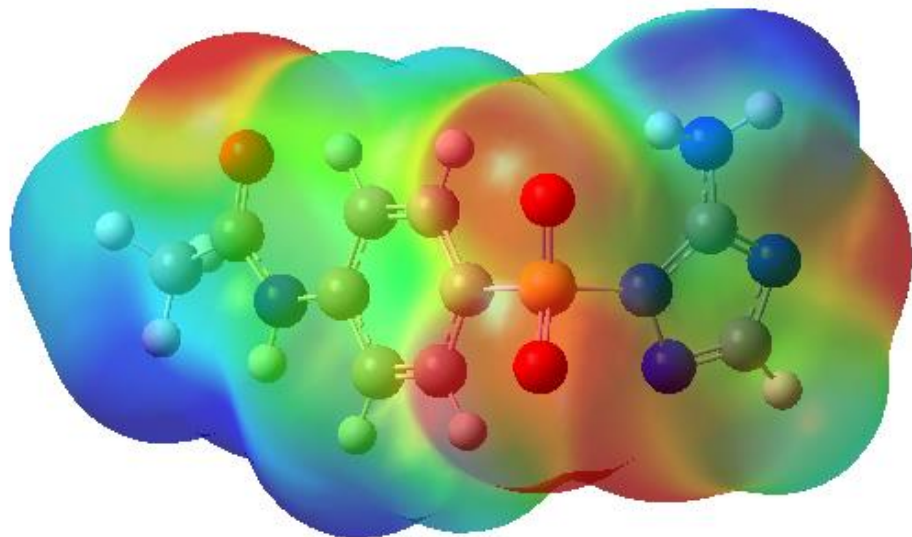


**Figure 3.** Map representation of the molecular electrostatic potential (MEP) surface.

### *3.3. Mulliken Charges*

Mulliken population analysis has been widely used to compute the charge distribution in molecules to identify the adsorption centers of inhibitors.

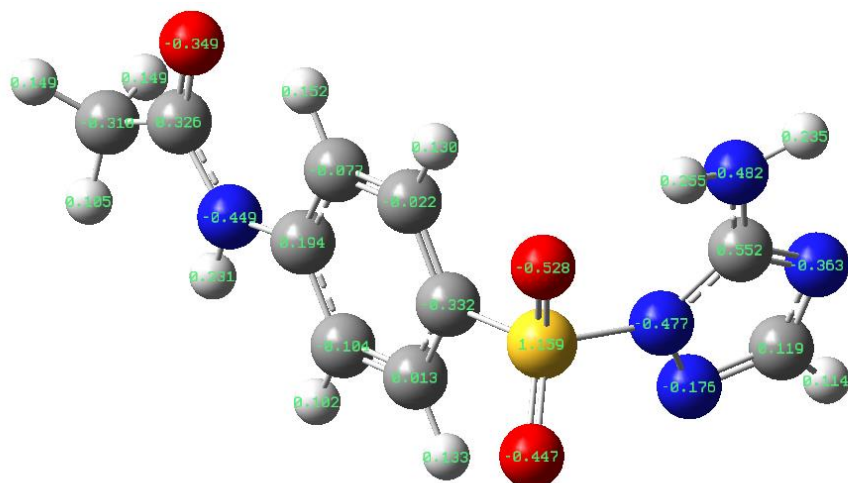


**Figure 4.** Mulliken atomic charge distribution of "4-Acetamido-N-(3-amino-1,2,4-triazol-1-yl) benzene sulfonamide" molecule

According to earlier studies, the atom with the higher negative atomic charge readily donates its electron to the metal's unoccupied orbital [45, 46]. Figure 4 illustrates the distribution of Mulliken atomic charges for the studied inhibitor.

It is evident that the most negative atomic charges are located on the carbon of the methyl group as well as on the oxygen and nitrogen atoms. These charge carriers serve as active centers for providing electrons to the metal surface. Further, the negative charges have a notable distribution along with the whole skeleton of the molecule, giving it high adsorption efficiency. In addition, it is important to realize that the inhibitor molecule can form a back donating bond with the copper atom's anti-bonding orbitals by receiving electrons from it [47].

### 3.4. Total and partial Density of states

A molecule's DOS represents the number of states occupied by it at a given energy range. In contrast, the PDOS clarifies the projection of specific orbitals on the energy scale for each molecular fragment or atom. The DOS and PDOS plots for the studied molecule are shown in Figure 5.

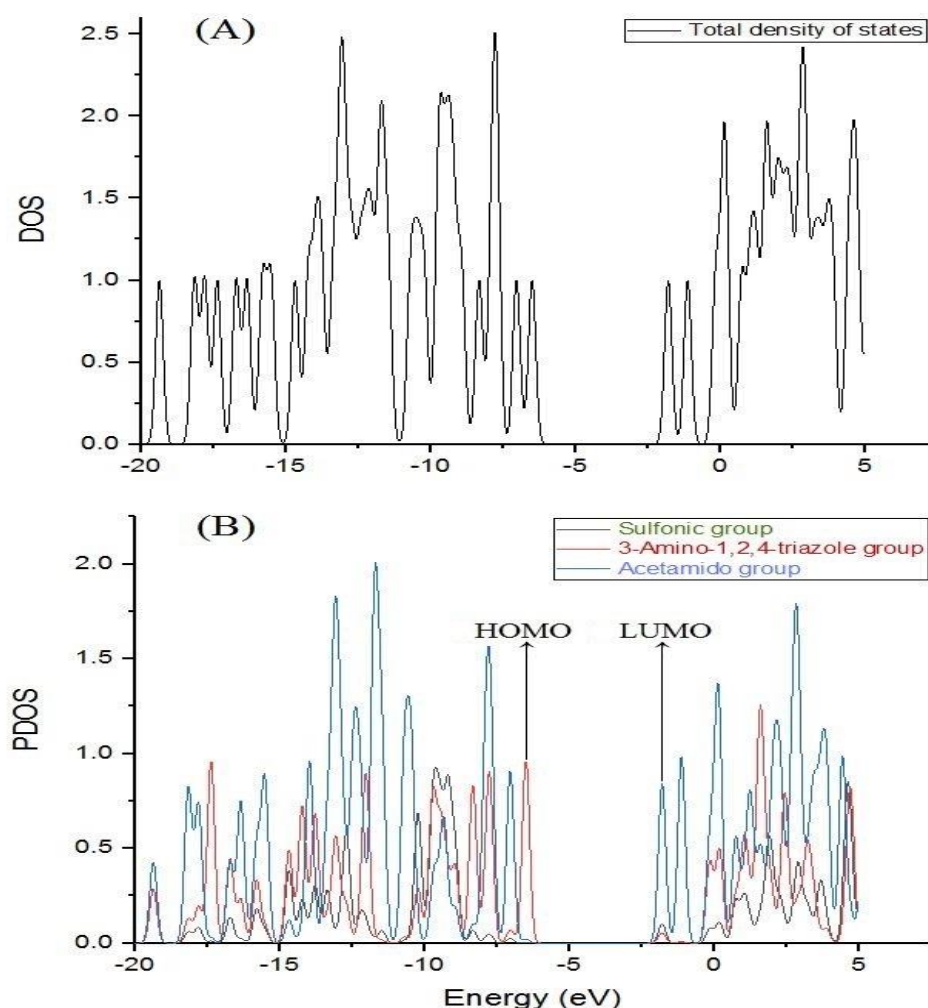


**Figure 5.** The diagram depicting the (A) DOS and (B) PDOS of "4-Acetamido-N-(3-amino-1,2,4-triazol-1-yl)benzenesulfonamide" molecule

The molecular orbital of 3-Amino-1,2,4-triazole entirely establishes the HOMO configuration. However, its orbital, on the other hand, is the main component of LUMO, with minor contributions from the sulfonic and the 3-Amino-1,2,4-triazole groups. The acetamido group clearly makes a significant contribution to the total DOS molecular orbitals. Hence, any alteration in this chain could easily affect the electronic properties of the molecule.

#### 4. CONCLUSION

DFT quantum computational modeling was used to investigate the electronic structure properties of the 4-acetamido-N-(3-amino-1,2,4-triazol-1-yl)benzenesulfonamide molecule and their relationship with corrosion inhibition performance. The calculated quantum reactivity indices, including the HOMO-LUMO energy gap, chemical hardness, softness, electronegativity, electrophilicity, and the fraction of electrons transferred, elucidated that the studied inhibitor has a high chemical reactivity.

The structural parameters were found to be consistent with the values found in the XRD literature. The frontier molecular orbitals disclosed the fragment offering/receiving electrons to interpret the electron transfer within the molecule. The MEP map and Mulliken charge distribution were used to distinguish active sites for nucleophilic/electrophilic attacks in addition to the locations of negative charges on the molecule surface. The DOS and PDOS were used to assess molecular orbital contributions.

The obtained results indicate desirable electronic properties, confirming the chemical reactivity of the proposed molecule and classifying it as a good candidate for copper corrosion inhibition.

#### References

1. Raafat M. Issa, Mohamed K. Awad and Faten M. Atlam, *Applied Surface Science*, 255 (2008) 2433.
2. Gerald Frankel et.al., *Faraday Discuss*, 180 (2015) 205.
3. Xiaogang Li, Dawei Zhang, Zhiyong Liu, Zhong Li, Cuiwei Du and Chaofang Dong, *Nature*, 527(2015) 441.
4. T.P.Chou. et. al., *journal of non-Crystalline Solids*, 290 (2001) 153.
5. Wail Al Zoubi and Young Gun Ko, *Scientific Reports*, 8 (2018) 10925.
6. Behzad Fotovvati, Navid Namdari and Amir Dehghanhadikolaei., *J. Manuf. Mater. Process*, 3 (2019) 28.
7. Chunxiao Chai, Yanhua Xu, Shuchen Shi, Xiaowei Zhao, Yufeng Wu, Ying Xu and Lei Zhang, *RSC Adv.*, 8 (2018) 24970.
8. Muhammad Shahid. *Adv. Nat. Sci.: Nanosci. Nanotechnol.*, 2 (2011) 043001.
9. K.F. Khaled, *Corrosion Science*, 52 (2010) 3225.
10. M. Mihit , K. Laarej , H. Abou El Makarim , L. Bazzi , R. Salghi and B. Hammouti, *Journal of Chemistry*, 3 (2010) 55.
11. K. Fukui and B. Pullman, *horizons of Quantum Chemistry*, (1980)5.
12. M. M. Antonijevic and M. B. Petrovic Int, *J. Electrochem. Sci.*, 3 (2008) 1.
13. Savaş Kaya and Cemal Kaya, *Molecular Physics*, 113 (2015) 1311.
14. Savas Kaya and Cemal Kaya, *Computational and Theoretical Chemistry*, 1060 (2015) 66.

15. Weitao Yang and Robert G Parr, *Proc. Nati. Acad. Sci. USA.*, 82 (1985) 6723.
16. Savas Kaya and Cemal Kaya, *Computational and Theoretical Chemistry*, 1052 (2015) 42.
17. Zaki S. Safia and Salama Omar, *Chemical Physics Letters*, 610 (2014) 321.
18. Pratim Kumar Chattaraj, UtpalSarkar and DebeshRanjan Roy, *Chem. Rev.*, 106 (2006) 2065.
19. Yon T. Koopmans, *Phys. Rev.*, 34 (1929) 1293.
20. A. K. Satpati and A. V. R. Reddy, *International Journal of Electrochemistry*, 2011(2011) 1.
21. I. Ahamad, R. Prasad, Eno E. Ebenso and M.A. Quraishi, *Int. J. Electrochem. Sci.*, 7 (2012) 3436.
22. M. Lashkari, M.R. Arshadi, *Chemical Physics*, 299 (2004) 131.
23. A.M. Deghady, R.K. Hussein, A.G. Alhamzani, A. Mera, *Molecules*, 26 (2021) 3631.
24. R. K. Hussein, H. M. Elkhair, A. O. Elzupir, K. H. Ibnaouf, *Journal of Ovonic Research*, 17 ( 2021) 23.
25. R. A. Hussein, I. I. Bashter, M. El-Okr, and M. Ibrahim, *Journal of Computational and Theoretical Nanoscience*, 13 (2016) 1.
26. Rageh K. Husseina, Ibrahim I. Bashter, Mohamed El-Okr and Medhat Ahmed Ibrahim. *Acta Chemical IASI*, 27(2019) 15.
27. K.H. Ibnaouf , R.K. Hussein, H.M. Elkhair , A.O. Elzupir. *Journal of Molecular Liquids*, 287 (2019) 110675.
28. V.V. Mehmeti and A.R. Berisha, *Front. Chem.*, 5(2017)61
29. Mwadham M Kabanda, Lutendo C. Murulana, MuzafferOzcan, FarukKaradag, IlyasDehri, I.B. Obot, Eno E. EbensoInt., *Int. J. Electrochem. Sci.*, 7 (2012) 5035.
30. Fadoua El Hajjaji, Mohammed E. Belghiti, MeriemDrissi, Mohammed Fahim, RajaeSalim, BelkheirHammouti, Mustapha Taleb and AyssarNahlé., *Portugaliae Electrochimica Acta*, 37(2019) 23.
31. F. Juan, Z. Chuan-Fang, S. Yu-Ting and H. Bo., *Acta Cryst.*, E63 (2007) o3116.
32. Krishnan Raghavachari., *Theor. Chem. Acc.*, 103(2000) 361.
33. Roland H. Hertwig, Wolfram Koch, *Physics Letters*, 268 (1997) 345.
34. M.j. Frisch, et.al, *Gaussian, Inc. Wallingford CT*, (2009).
35. R. Dennington, T. Keith and J. Millam, *Gauss View, Semichem Inc.*, Shawnee Mission, KS, (2009)
36. N. M. O'boyle, A. Tenderholt and K. M. Langner, *J Comput Chem.*, 29 (2008) 839.
37. Takao Tsuneda, Jong-Won Song, Satoshi Suzuki, and KimihikoHirao., *The Journal of Chemical Physics*,133 (2010) 174101.
38. Anton Kokalj , *Corrosion Science*, 193 (2021) 109650.
39. Jiayul Haque, Vandana Srivastava, ChandrabhanVerma, M.A. Quraishi., *Journal of Molecular Liquids*, 225 (2017) 848.
40. Dmitry Shevtsov, et.al. *Appl. Sci.*, 9 (2019) 4882.
41. P. Geerlings and F. De Proft., *Int. J. Mol. Sci.*, 3(2002) 276.
42. L.R. Dewar, M.J. Aurell, P.Perez, R. Contreras, *Tetrahedron*, 58 (2002) 4417.
43. M.J.S. Dewar, E. G. Zoebisch, E. F. Heali and J.J.P.Stewart., *J. Am. Chem. Soc.*, 107(1985) 3902.
44. G. Velraj , S. Soundharam. *Journal of Molecular Structure*, 1074 (2014) 475.
45. H. Shokry , E.M. Mabrouk. *Arabian Journal of Chemistry*, 10 (2017) S3402.
46. Sourav Kr. Saha and Priyabrata Banerjee. *The Royal Society of Chemistry*, 00 (2012) 1.
47. N.O. Obi-Egbedi, I.B. Obot, M.I. El-Khaiary, S.A. Umoren and E.E. Ebenso. *Int. J. Electrochem. Sci.*, 6 (2011) 5649.